Mutational analysis of Mei5, a subunit of Mei5-Sae3 complex, in Dmc1-mediated recombination during yeast meiosis

Stephen Mwaniki[1,2], Priyanka Sawant[1,2, 3], Osaretin P. Osemwenkhae[1,4], Yurika Fujita[1], Masaru Ito[1], Asako Furukohri[1], and Akira Shinohara[1, *]

[1]Institute for Protein Research, Osaka University, Suita, Osaka 565-0871, Japan

Short title: Mutational analysis of yeast Mei5

Keywords: meiotic recombination, Dmc1, Rad51, Mei5-Sae3, cleavage

[2]Contributed equally
[3]Present address: Takeda Pharm. Co. Ltd.
[4]Present address: University of Benin, Nigeria

*Corresponding author:
Akira Shinohara
Institute for Protein Research, Osaka University
3-2 Yamadaoka, Suita, Osaka 565-0871 JAPAN
Phone: 81-6-6879-8624
FAX: 81-6-6879-8626
E-mail: ashino@protein.osaka-u.ac.jp
ORCID: 0000-0003-4207-8247

Abstract

Interhomolog recombination in meiosis is mediated by the Dmc1 recombinase. The Mei5-Sae3 complex of *S. cerevisiae* promotes Dmc1 assembly and functions with Dmc1 for homology-mediated repair of meiotic DNA double-strand breaks. How Mei5-Sae3 facilitates Dmc1 assembly remains poorly understood. In this study, we created and characterized several *mei5* mutants featuring the amino acid substitutions of basic residues. We found that Arg97 of Mei5, conserved in its ortholog, SFR1(complex with SWI5), RAD51 mediator, in humans and other organisms, is critical for complex formation with Sae3 for Dmc1 assembly. Moreover, the substitution of either Arg117 or Lys133 with Ala in Mei5 resulted in the production of a C-terminal truncated Mei5 protein during yeast meiosis. Notably, the shorter Mei5-R117A protein was observed in meiotic cells but not in mitotic cells when expressed, suggesting a unique regulation of Dmc1-mediated recombination by post-translational processing of Mei5-Sae3.

Introduction

Meiotic recombination plays a critical role in chromosome segregation in meiosis I and in generating a new combination of alleles in gametes for diversity (Borner, Hochwagen, & MacQueen, 2023; Marston, 2014). The recombination promotes reciprocal exchange between homologous chromosomes creating physical linkages between them, rather than between sister chromatids (Cejka, Mojas, Gillet, Schar, & Jiricny, 2005; Hunter, 2015). This interhomolog bias is regulated by modulating the recombination machinery as well as chromosome structure during meiosis.

Meiotic recombination in the budding yeast, *S. cerevisiae*, is induced by the formation of DNA double-strand breaks (DSBs), followed by the generation of single-stranded DNA (ssDNA) through end processing. Two RecA homologs, Rad51 and Dmc1 (Bishop, Park, Xu, & Kleckner, 1992; A. Shinohara, Ogawa, & Ogawa, 1992) form a nucleoprotein filament on the ssDNA for homology search and strand exchange between the ssDNA and a homologous double-stranded DNA (dsDNA) (Luo et al., 2021; Ogawa, Yu, Shinohara, & Egelman, 1993; Xu et al., 2021). In meiosis, Rad51 plays a non-catalytic, structural role in interhomolog recombination by aiding the assembly of Dmc1 filament (Cloud, Chan, Grubb, Budke, & Bishop, 2012; Lan et al., 2020) while Rad51 catalyzes the intersister

strand exchange in mitosis. The Dmc1 filament catalyzes the interhomolog strand exchange. The assembly of Rad51 filament on ssDNAs coated with a ssDNA-binding protein, Replication protein A (RPA) is tightly regulated by Rad51 mediators: Rad52, Rad55-Rad57, and Psy3-Csm2-Shu1-Shu2 in the budding yeast (Sasanuma et al., 2013; A. Shinohara & Ogawa, 1998; Sung, 1997). On the other hand, Dmc1 assembly on RPA-coated ssDNAs is promoted by the meiosis-specific complex, Mei5-Sae3, as well as Rad51 (Chan, Zhang, Weissman, & Bishop, 2019; Ferrari, Grubb, & Bishop, 2009; Hayase et al., 2004; Tsubouchi & Roeder, 2004).

The budding yeast Mei5-Sae3 belongs to a family of protein complexes along with Sfr1-Swi5 in the fission yeast, which regulates the assembly of both Rad51 and Dmc1 filaments (Akamatsu, Dziadkowiec, Ikeguchi, Shinagawa, & Iwasaki, 2003). Sfr1-Swi5 and Mei5-Sae3 complexes are conserved from yeast to mammals (Akamatsu et al., 2007; Hayase et al., 2004; Tsai et al., 2012). Fission yeast and mouse Sfr1-Swi5 promote both Rad51-mediated strand exchange *in vitro* by stabilizing an active ATP-bound form of Rad51 filaments (Chi et al., 2009; Haruta et al., 2008). Consistent with this, structure studies showed that the C-terminal region of Sfr1 (Sfr1C), when complexed with Swi5, forms a kinked rod, that may fit into a groove of the Rad51 filament (Kokabu et al., 2011; Kuwabara et al., 2012). Swi5 and Sae3 encoding small proteins with fewer than 100 amino acids (aa), are homologous to each other (Akamatsu et al., 2007; Hayase et al., 2004). On the other hand, Mei5 and Sfr1 are highly divergent showing limited homology (Hayase et al., 2004). Still how the formation of the Mei5-Sae3 complex is regulated in a meiotic cell is largely unknown.

Given that Mei5-Sae3 binds to ssDNA (Ferrari et al., 2009; Say et al., 2011), we constructed several *mei5* mutants in which a positively-charged amino acid is replaced with neutral amino acids, alanine or leucine, and characterized the meiotic phenotypes of the mutants. We showed that Arg97 in the conserved KWR motif of the Mei5/Sfr1 family is critical for the binding to Sae3. We also found that the substitution of either Arg117 or Lys133 with alanine produced a C-terminal truncated Mei5 protein (Mei5-R117A and Mei5-K133A, respectively), suggesting the presence of post-translational processing of the mutant Mei5 proteins. The role of post-translational processing is discussed.

Results

Mutational analysis of Mei5

100 Previous study showed a crystal structure of fission yeast Swi5 complex with
101 Sfr1C (N-terminal truncated version of Sfr1) (Kuwabara et al., 2012) (PDB, 3viq).
102 Amino acid sequence comparison revealed weak similarity between the budding
103 yeast Mei5 and fission yeast Sfr1 (Hayase et al., 2004). In the sequence, regions
104 of α1 and α2 of the Sfr1 protein are more homologous to those in Mei5. α1 and
105 α2 of the Sfr1 protein form parallel α-helixes with two α-helixes of Swi5
106 (Kuwabara et al., 2012). Indeed, the AlphaFold2 prediction (Jumper et al., 2021)
107 showed that Mei5 contains four α-helixes followed by two short α-helixes (Figure
108 1A). Two α-helixes (α1 and α2) of the N-terminal of Mei5 share the structural
109 similarity to the two helixes of Sfr1 (Figure 1B). On the other hand, the predicted
110 C-terminal region of Mei5, which contains anti-parallel α-helixes followed by two
111 short α-helixes is different from the C-terminal Sfr1 with anti-parallel β-sheet
112 followed by a short α-helix (Figure 1B).
113 We were interested in the function of the conserved α-helixes, the α1 and
114 α2 of Mei5. Particularly, the α2 bears highly conserved KWR/K motif among
115 Sfr1/Mei5 orthologues (Supplementary Figure S1A, B). Since a purified Mei5-
116 Sae3 binds to ssDNAs (Ferrari et al., 2009; Say et al., 2011), we focused on
117 positively-charged amino acids in the α1 and α2 of Mei5; Lys51, Arg58, Arg68,
118 Lys79, Arg90, Lys91, Lys95, Arg97, Lys114, and Arg117 (Mei5 in SK1 strain is
119 one amino acid shorter than that in other strains-Glu17, Glu18 in SK1 instead of
120 Glu17, Glu18, Glu19 in others) and Lys95 and Arg97 are in the KWR/K motif
121 (Figure 1A, left). We substituted the lysine or arginine with either alanine or
122 leucine in 7 (9) mutants; *mei5-K51A R58A* (double mutant), *mei5-R68A K79A*
123 (double mutant), *mei5-R90A K91A* (double mutant), *mei5-K95A* (and *-K95L*),
124 *mei5-R97A* (and *-R97L*) *mei5-K114A*, and *mei5-R117A* in the SK1 background.
125 The staining of the cells with a DNA-binding dye, DAPI, reveals that, after
126 synchronous induction of meiosis, *mei5-R68A K79A*, *mei5-K95L*, and *mei5-*
127 *K114A* showed similar timing of the entry of meiosis I to that in the wild-type cells
128 (Figure 1C). The *mei5-K51A R58A* showed ~1 h delay in the entry into MI. The
129 *mei5-K95A* mutant cells delayed ~4 h in the entry in meiosis I while the *mei5-*
130 *K95L* cells showed normal MI progression. Moreover, except for the *mei5-K95A,*
131 the mutant cells expressed Mei5 proteins with expression kinetics similar to wild-
132 type Mei5 protein, which appears at 2 h and increases in its level in further
133 incubation (Figure 1D and Supplementary Figure S1C). The *mei5-K95A* delayed
134 the expression of Mei5 with a reduced level relative to the wild-type (Figure 1D).
135 The *mei5-K95L* mutant followed a similar expression pattern to the wild-type Mei5.

136 The delayed meiosis I in the *mei5-K95A* would be due to the delayed expression
137 of the Mei5-K95A protein (Figure 1D). Although the *mei5-K51A R58A* showed a
138 slight delay in MI progression, the spore viability of the *mei5-K51A R58A* mutant
139 is at a wild-type level with 97.0% (97.8% in wild-type). The spore viability of the
140 *mei5-K95A* mutant is 96.5%.
141 We further characterized *mei5-K95L*, *-R97A*, *-R97L*, and *-R117A* mutants
142 in more detail.
143 **The *mei5-K95L* mutant:** To know the role of highly-conserved Lys95 among
144 Mei5/Sfr1, we further characterized the *mei5-K95L* mutant, which shows normal
145 expression of Mei5 protein in detail. Moreover, immuno-staining analysis of
146 Rad51 on chromosome spreads revealed the normal appearance of Rad51-
147 positive spreads (Figure 2A, B) but a slight delay in the disappearance of Rad51
148 in the mutant (Figure 2C). The *mei5-K95L* mutant delayed the appearance and
149 disappearance of Dmc1 slightly compared to the wild-type. The peak value of
150 Dmc1-positive cells at 4 h is lower than that in the wild-type (Figure 2C). The
151 Dmc1-focus number in the mutant is lower than that in the wild-type (19.1 in the
152 mutant at 4 h while 33.0 in the control; Figure 2D and Supplementary Figure S2B).
153 These indicate that the *mei5-K95L* mutant bears a weak defect in the Dmc1
154 assembly. Mei5 staining revealed that the Mei5 foci appeared with a slight delay,
155 peaked at 4 h, and disappeared at the normal timing. The number of Mei5 mutant
156 foci is 21.4 at 4 h, which is lower than that of wild-type Mei5 foci (29.4). Given
157 that the *mei5-K95L* mutant slightly decreased the spore viability to 91.7%
158 compared to the control (97.8%), Lys95 is not essential for Mei5 function *in vivo*.
159 A non-essential role of the highly-conserved residue(s) is also seen in Tyr56 of
160 the conserved YNEL sequence of the Mei5 partner, Sae3 (Sawant et al., 2023).
161
162 **The *mei5-R97A* and *-R97L* mutants were partially deficient in Dmc1**
163 **assembly**
164 The *mei5-R97A* and *-R97L* mutants showed an arrest in meiotic prophase I
165 (Figure 1C). Like the *mei5* deletion mutant, these mutants formed Rad51 foci
166 normally like in the wild-type strain but accumulated the foci as meiosis
167 progresses (Figure 2), suggesting stalled recombination. This is confirmed by the
168 accumulation of Rfa2 (the second subunit of RPA) foci (Supplementary Figure
169 S2A) The kinetics of Rfa2 foci in both of the mutants are similar to those of Rad51
170 foci (Figure 2C and D). Moreover, the chromosomal fragmentation analysis by
171 the CHEF (Counter-clamped homogeneous electric field) gel electrophoresis

172 confirmed the accumulation of fragmented chromosomes induced by meiotic
173 DSBs in the *mei5-R97L* mutant as seen in the *mei5* deletion mutant
174 (Supplementary Figure S3C)**.**
175 Dmc1 staining revealed that the *mei5-R97A* and *-R97L* mutants are partially
176 defective in Dmc1-focus formation (Figure 2A, C and D). At early time points such
177 as 3 and 4 h, the appearance of Dmc1 foci in both mutants is delayed relative to
178 the wild-type control. Moreover, at 10 and 12 h, only ~40% of mutant cells were
179 positive for the Dmc1 foci, suggesting a defect in Dmc1 disassembly. The steady-
180 state number of Dmc1 foci per spread in the *mei5-R97L* mutant is 10.7 and 14.4
181 at 4 and 8 h, respectively while that in the wild-type is 33.0 at 4 h (Supplementary
182 Figure S2B), consistent with that the *mei5-R97L* mutant is defective in Dmc1
183 assembly. The mutant accumulated Dmc1 foci at late times in meiosis. Therefore,
184 the Dmc1 complex formed in the *mei5-R97A* and *-R97L* cells is likely to be
185 functionally defective.
186 The Mei5 staining revealed a defective assembly of Mei5 in the *mei5-R97A*
187 and *-R97L* cells (Figure 2B, C and D). At early time points such as 3, 4, and 5 h,
188 we could not detect a clear signal of Mei5 on the spreads. After 6 h, Mei5 foci
189 started to appear and accumulated with ~50% of cells positive for Mei5 during
190 further incubation. On the other hand, the number of Mei5 foci in the *mei5-R97L*
191 mutant was 10.2 and 9.8 at 6 and 8 h, respectively, which is lower than that of
192 Mei5 foci in the wild type (29.4 at 4 h). These suggest that the Dmc1 assembly in
193 the *mei5-R97A and -R97L* mutants occurs without visible Mei5-focus formation.
194 Moreover, it seems that the mutant Mei5-R97L/A protein could bind to a pre-
195 assembled Dmc1 ensemble.
196
197 **Arg97 in Mei5 protein is required for efficient complex formation with Sae3**
198 To know the interaction of the Mei5-R97L protein with Sae3, we introduced the
199 *SAE3-Flag* allele, which is functional (Hayase et al., 2004; Sawant et al., 2023),
200 in the *mei5-K95L* and *mei5-R97L* mutants. Like the *mei5-R97L*, *mei5-R97L*
201 *SAE3-FLAG* cells, which expressed both Mei5 and Sae3 protein as seen in the
202 wild-type (Supplementary Figure S3A) were arrested at meiosis I and
203 accumulated Rad51 and Rfa2 foci (Figure 3A, C, Supplementary Figure S3B). As
204 seen in the *mei5-R97L*, *mei5-R97L SAE3-FLAG* mutant accumulated meiotic
205 DSBs (Supplementary Figure S3D), indicating defective processing of
206 recombination intermediates. Distinct from *mei5-R97L*, the *mei5-R97L SAE3-*
207 *FLAG* mutant is almost defective in Dmc1-focus formation (Figure 3A and C;

208 compare with Figure 2A), indicating a genetic interaction between the *mei5-R97L*
209 and *SAE3-Flag* alleles. The number of Dmc1 foci in the mutant is 2.3 and 3.0 at
210 6 and 8 h, respectively (Figure 3D and Supplementary Figure S4). Moreover, the
211 focus formation of both Mei5 and Sae3-Flag is fully impaired in the mutant (Figure
212 3B).
213 We performed the immuno-precipitation (IP) of the Sae3-Flag protein in
214 meiotic yeast cell lysates. From *SAE3-FLAG* cells, the IP using anti-Mei5 pulled
215 down the Sae3-Flag protein efficiently (Figure 3E). On the other hand, the IP of
216 Mei5-R97L did not reveal the Sae3-Flag protein while Mei5-W96A, which is the
217 amino acid substitution of Trp96 next to Arg97, showed the complex formation
218 with Sae3-Flag (Figure 3E). These showed that conserved Arg97 of Mei5 is
219 critical for Mei5-Sae3 complex formation.
220 Although the *mei5-K95L* mutant behaves almost like wild-type (Figure 2),
221 when combined with the *SAE3-Flag*, it showed a clear defect in the assembly and
222 disassembly of Dmc1 (Figure 3A, C and Supplementary Figure 3A). The focus
223 formation of Mei5 and Sae3-Flag is clearly reduced in the strain compared to the
224 *SAE3-Flag* cells (Figure 3B, C, D, and Supplementary Figure S4). Mei5-K95L
225 mutant protein can form a complex with Sae3-Flag (Figure 3E). These support
226 the idea that the C-terminal tagging of Sae3 affects the function and also that the
227 *mei5-K95L* substitution weaken the function of Mei5(-Sae3).
228
229 **The *mei5-R117A* mutant produced a shorter Mei5 protein**
230 Like the *mei5* null mutant, the *mei5-R117A* mutant, which is arrested in meiosis I
231 (Figure 1B), is defective in Dmc1-focus formation but proficient in focus formation
232 of Rad51 (Figure 4A and C). Rad51 foci persisted as meiosis progresses (Figure
233 4C). Immuno-staining of Mei5 revealed very few detectable Mei5 foci in *mei5-*
234 *R117A* cells (Figure 4B and C). Arg117 is essential for the Mei5 function.
235 On the other hand, on western blots using anti-Mei5 anti-serum, Mei5-
236 R117A protein migrated as much faster bands at the position of around 25kD
237 while wild-type protein (221 aa protein with calculated MW of 26 kD) ran at ~30kD
238 position (Figure 1C and 5A). Time course analysis showed that short-forms of
239 Mei5-R117 protein as two bands appear at 2 h after the induction of meiosis,
240 which is similar timing of the expression of the wild-type Mei5 protein. The shorter
241 forms of Mei5-R117 protein are stable, which were detectable at late time points
242 such as 10 h.
243 There are two possibilities for the formation of the shorter Mei5-R117 protein

244 on the blot. First, wild-type Mei5 protein is post-translationally modified to the
245 protein with a larger molecular weight than the unmodified protein. Indeed, Mei5
246 is SUMOylated at Lys56 (Bhagwat et al., 2021). Second, the mutant protein is
247 subject to the processing after synthesized as a full-length protein. We compared
248 the mobility of Mei5 protein expressed in meiotic yeast cells with purified Mei5(-
249 Sae3) protein produced in *E. coli* (Hayase et al., 2004) and found the mobility of
250 yeast Mei5 is similar to that Mei5 from *E. coli* (Figure 5A and C), suggesting that
251 wild-type Mei5 protein is unlikely to be subject to the modification which induces
252 the change of molecular weight on the gel. To confirm the processing of Mei5-
253 R117A protein, we added the 3XFlag tag at the C-terminus of Mei5 protein. Wild-
254 type Mei5-Flag protein was detected on blots as a band with a similar molecular
255 weight (~35kD) by using both anti-Mei5 and anti-Flag antibodies (Figure 5B). On
256 the other hand, anti-Mei5 antiserum detected Mei5-Flag protein in *mei5-R117A-*
257 *Flag* cell lysates, whose size is ~20kD, similar to Mei5-R117A (Figure 5B, right),
258 indicating that the C-terminal Flag did not affect the size of Mei5-R117A protein.
259 Moreover, the anti-Flag antibody could not detect the Mei5-R117A mutant protein
260 with ~20kD (Figure 5B, left). These suggest that the C-terminal region is missing
261 on the Mei5-R117A band. Moreover, there is a weak signal of full-length Mei5-
262 R117A-Flag protein in the lysates, which is prominent at 6 h, implying the post-
263 translational processing of a full-length Mei5-R117A-Flag protein. Of note, we
264 often detected smaller bands of wild-type Mei5, which migrated almost similar
265 two bands Mei5-R117A protein (red arrowhead in Figure 5A and B; the ratios of
266 the two bands are different between wild-type Mei5 and Mei5-R117A).
267 We expressed Mei5-R117A protein with Sae3 from *E. coli* cells and found
268 the size of Mei5-R117A in *E. coli* lysates is similar to that of wild-type Mei5 protein
269 expressed in *E. coli* (Figure 5A, C and Supplementary Figure S5). It is unlikely
270 that the auto-cleavage activity of Mei5-R117A, supporting the idea that Mei5-
271 R117A is subject to the processing in yeast.
272
273 **Mei5-R117A protein undergoes meiosis-specific posttranslational**
274 **processing**
275 To estimate the possible truncated position in the C-terminus of Mei5-R117A, we
276 constructed the *mei5-d(190-221)* and *mei5-d(197-221)* mutants which lacked the
277 C-terminal 32 and 25 aa, respectably, and compared the migration of these C-
278 terminal truncated proteins with Mei5-R117A (Figure 6A). Mei5-R117A migrated
279 a bit faster than these truncated Mei5 proteins (Figure 6B). This suggests that the

280 possible cleavage might occur around 190 residues of Mei5 (see blue region of
281 a putative Mei5 structure in Figure 1A). Like the *mei5* deletion mutant, the *mei5-*
282 *d(190-221)* and *mei5-d(197-221)* mutants arrest during meiotic prophase I
283 (Figure 6C), indicating that the C-terminal two small α-helixes (α5 and α6) are
284 critical for the Mei5 function.
285 To know the requirement of the post-translational processing of Mei5-
286 R117A, we constructed additional substitutions of Arg117 with lysine and
287 glutamate, *MEI5-R117K* and *-R117E*, respectively. When we checked the size of
288 these versions of Mei5, both Mei5-R117K and -R117E exhibited a similar size of
289 the wild-type protein (Figure 6D). Indeed, in contrast to *mei5-R117A, MEI5-*
290 *R117K* and *-R117E* cells showed normal MI progression with wild-type spore
291 viability: wild-type, 97.1% (52 tetrads), *MEI5-R117K*, 97.5% (50 tetrads) and
292 *MEI5-R117E*, 95.0% (5 tetrads: Figure 6E). Although we have not tested other
293 substitutions of Arg117, the substitution to alanine is critical for the processing.
294 Given some protein processing in yeast depends on the proteasome, we
295 treated the meiotic wild-type cells with a proteasome inhibitor, MG132 and the
296 treatment with MG132 did not affect the mobility of Mei5-R117A as well as wild-
297 type Mei5 (Supplementary Figure S6). The processing of Mei5-R117A seems to
298 be independent of the proteasome.
299 We checked the complex formation of Mei5-R117A with Sae3 is necessary
300 for the processing (Figure 6F). Like the *mei5-R117A* mutant, the *mei5-R117A*
301 mutant with the *SAE3* deletion generated the truncated Mei5 protein. In the
302 absence of Sae3, the Mei5-R117A protein is less stable relative to that in the
303 presence of wild-type Mei5. Moreover, we expressed Mei5-R117A protein in
304 mitotic yeast cells, which do not express Sae3, by putting it under the control of
305 the *GAL1/10* promoter (which is defective for the induction in the SK1 strain).
306 Mitotically-expressed Mei5-R117A protein migrated at the same position as wild-
307 type Mei5 (Figure 6G). This suggests that the processing of Mei5-R117A protein
308 is specific to meiosis.
309
310 **K133A substitution of Mei5 also induces meiosis-specific posttranslational**
311 **processing**
312 The R117A substitution might change the structure of Mei5, which makes it
313 sensitive to a cellular protease. However, the Alphafold2 prediction (Jumper et
314 al., 2021) showed that a predicted structure of Mei5-R117 is almost same to that
315 of wild-type Mei5 (Supplementary Figure S7A). Moreover, we extended our

316 mutational analysis to the basic residues in the α3 helix of Mei5 (Figure 7A),
317 which is not conserved among the Mei5/Sfr1 family (Figure 1B), We found that
318 the Lys133 substitution to Alanine also produced a shorter version of Mei5, whose
319 size is similar to that of Mei5-R117A protein (Figure 7B). Again, the Alphafold2
320 prediction showed that K133A did not affect the Mei5 structure (Supplementary
321 Figure S7B). Moreover, the substitution of Arg134, next to Lys133, with Alanine
322 did not affect the production of a full-length Mei5-R134A protein. Therefore, it is
323 likely that the Mei5 protein contains some amino acid residues such as Arg117
324 and Lys133, which protects the protein from post-translational processing.
325
326 **Discussion**
327 Mei5-Sae3 promotes Dmc1 assembly in the budding yeast. Previous biochemical
328 studies show that Mei5-Sae3 promotes Dmc1-mediated D-loop formation by
329 overcoming the inhibitory effect of RPA on Dmc1 assembly on the ssDNA (Chan
330 et al., 2019; Cloud et al., 2012). How Mei5-Sae3 helps Dmc1 assembly on ssDNA
331 remains largely unknown. The biochemical analysis of fission yeast and mouse
332 Sfr1-Swi5, an ortholog of Mei5-Sae3, provides some mechanistic insight into how
333 the complex promotes Rad51 assembly. Fission yeast and mouse Sfr1-Swi5
334 stabilizes ATP-bound form of Rad51 on ssDNAs (Haruta et al., 2006; Su et al.,
335 2014). The structural analysis suggests that the fission yeast Sfr1-Swi5 binds to
336 a groove of Rad51 filament (Kuwabara et al., 2012). Although we analyzed the
337 role of conserved residues of Sae3 in the yeast meiosis (Sawant et al., 2023), the
338 contribution of conserved amino acids in Mei5 has not been analyzed. Here, we
339 characterized the substitution of basic amino acids on putative conserved α-
340 helixes of Mei5 protein and identified key residues for *in vivo* Mei5 function.
341
342 **The role of conserved KWR motif in Mei5/Sfr1 family**
343 The Mei5/Sfr1 orthologs are poorly conserved at the amino acid sequence.
344 Among them, the KWK/R (Lys95-Trp96-Arg97) in the putative α2 helix in Mei5 is
345 conserved among the family. In fission yeast Sfr1(-Swi5), the three residues are
346 not involved in the binding with Swi5, rather are located on the surface of the
347 complex (Supplementary Figure S1A). While the substitution of Lys95 did not
348 affect Mei5 function *in vivo*, the substitution of Arg97 impaired the function.
349 Although Mei5-R97L cannot form a complex efficiently *in vivo*, the protein might
350 have a reduced Dmc1-assembly activity, suggesting that a stable complex
351 between Mei5 and Sae3 is unnecessary for the function of the complex. While

352 Mei5-R97L (and -R97A) can recruit Dmc1 on meiotic chromosomes, Dmc1
353 assembly occurs before the Mei5 assembly in the *mei5-K95A/L* mutant. This
354 suggests that a stoichiometric amount of Mei5-Sae3 relative to Dmc1 is not
355 necessary for the role of the complex as the Dmc1 mediator. In other words, a
356 small amount of Mei5-Sae3 is sufficient for Dmc1 assembly.
357 In wild type, the loading of Dmc1 and Mei5-Sae3 is mutually inter-dependent
358 (Hayase et al., 2004; Tsubouchi & Roeder, 2004). Interestingly, Mei5-R97A/L
359 binds on meiotic chromosomes later than Dmc1, suggesting that the loading of
360 Mei5-Sae3 is temporally separable from Dm1 loading. Moreover, Mei5(-R97A/L)-
361 Sae3 seems to be able to bind to a pre-assembled Dmc1 complex. This implies
362 the role of Mei5-Sae3 in post-assembly stage of Dmc1 filament such as the
363 stabilization of the filament as proposed to the fission yeast and mouse Sfr1-Swi5
364 (Haruta et al., 2006; Lu et al., 2018).
365 The *mei5-K95L* mutant alone is almost normal in Dmc1 assembly. On the
366 other hand, the combination of the substitution with the *SAE3-Flag* makes this
367 Mei5-Sae3 complex defective in the assembly of Dmc1 as well as the loading of
368 Mei5 and Sae3 (Figure 3C). This suggests a possible role of Lys95 in Mei5
369 function. The position of KWR motif of fission yeast Sfr1 is near the C-terminus
370 of Swi5 on the predicted structure (Kuwabara et al., 2012) (Supplementary Figure
371 S1), supporting the idea of the functional cooperation of the KWR motif of Mei5
372 with Sae3 C-terminus.
373
374 **Possible post-translational processing of Mei5-R117A and -K133A proteins**
375 Arg117 substitution with Ala but not Lys or Glu induced the post-translational
376 cleavage of the mutant Mei5 protein, which could generate Mei5 protein deleted
377 for the C-terminal ~30 amino acids. Since the two C-terminal deletion *mei5*
378 mutants, *mei5-d(190-221)* and *mei5-d(197-221)*, are defective in meiosis, we
379 speculate that the processing inactivates the Mei5 function. Although we do see
380 the robust cleavage of Mei5-R117A protein *in vivo*, we do not have clear evidence
381 that wild-type Mei5 is a target for the similar post-translational processing. In wild-
382 type cells, we detected that Mei5 protein with a similar size to processed Mei5-
383 R117A in addition to full-length Mei5, although the amount of the processed
384 proteins is relatively very small compared to that of a full-length Mei5 protein (see
385 bands with read arrowheads in Figure 6B). This suggest that the wild-type Mei5
386 is subject to the similar processing to Mei5-R117A protein, although less sensitive
387 compared to the mutant protein. So even if such the processing may exist for

388 wild-type Mei5 protein, it does not seem to operate under a laboratory optimized
389 condition of meiosis.
390 One likely idea is that R117A substitution affect a structure of Mei5, which
391 sensitizes the mutant protein to the protease. Mei5-Arg117 is located in the α2
392 helix while the processing seems occur in a structurally distinct region (α4; Figure
393 1A). Importantly, the Alphafold2 prediction showed R117A substitution did not
394 affect the Mei5 structure (Supplementary Figure 7A). Moreover, in addition to
395 R117A substitution, we found the second substitution, K133A, also induced the
396 Mei5 processing. The Alphafold2 prediction showed that K133A does not affect
397 the Mei5 structure (Supplementary Figure 7B). Lys133 of Mei5 resides in the
398 independent structure from that with Arg117. We suggest that Mei5 evolves
399 amino acid residues such as Arg117 and Lys133, which protects the protein from
400 post-translational processing in yeast meiotic cells.
401 The processing of Mei5-R117A is rapid and under the control of biologically
402 regulated process, since we see the cleavage of the mutant Mei5 only in meiotic
403 cells, but not in mitotic cells. There are limited reports on post-translational
404 processing of the protein in the budding yeast, although such the phenomenon is
405 often reported in multi-cellular organism. In the budding yeast, the membrane-
406 bound Mga2 transcriptional factor p120 is converted into un-anchored Mga2-p90,
407 which is imported to the nucleus for the transcriptional regulation in mitotic cells
408 (Bhattacharya et al., 2009; Hoppe et al., 2000). This processing depends on the
409 proteasome and Cdc48 unfoldase. In meiosis, nuclear envelope protein, Mps3,
410 is cleaved in its N-terminal ~90 amino acids by the proteasome-dependent
411 mechanism only in a specific window of late meiotic prophase I (Li et al., 2017).
412 The cleavage of Mei5-R117A might be related to these reported processes.
413 However, the proteasome inhibitor, MG132, treatment did not inhibit the
414 appearance of Mei5-R117A. It is likely that the processing of Mei5-R117A is
415 proteasome-independent. To elucidate the biological role of this processing as
416 well as to get the mechanical insight, the identification of Mei5 residues (or
417 regions) necessary for the cleavage or the cleavage site(s) as well as the
418 protease mediating the process is necessary.
419
420 **Experimental Procedures**
421 **Strains**
422 All strains described here are derivatives of SK1 diploids, NKY1551 (*MATα/MAT**a**,*
423 *lys2/", ura3/", leu2::hisG/", his4X-LEU2-URA3/his4B-LEU2, arg4-nsp/arg4-bgl*).

424 The genotypes of each strain used in this study are described in Supplemental
425 Table S1.
426
427 **Strain Construction**
428 The *mei5* mutant genes were constructed by the pop-in/pop-out method. PCR-
429 based site-directed mutagenesis was carried out using the yIPlac195 plasmid
430 with wild-type *MEI5* gene as a template. The sequence of primer DNAs using
431 site-directed mutagenesis is provided in Supplementary Table S2. DNA changes
432 were confirmed by Sanger DNA sequencing. The plasmids with the mutant *MEI5*
433 gene were introduced in the yeast haploid strain of MSY832 by transformation
434 with litium acetate and yeast cells were selected for uracil prototroph. The
435 presence of the mutants was confirmed by the restriction digestion of PCR
436 products. The candidate yeast cells were grown overnight in YPAD liquid culture
437 and were plated on a selection media containing 5-FOA (5-fluoroortic acid) for
438 uracil auxotroph. The C-terminal *mei5* deletion mutants were constructed by
439 PCR-mediated one-step replacement using pFA6a-KamMX4. The primer
440 sequences are provided in Supplemental Table S2. The deletions were confirmed
441 again by restriction digestion of PCR products and the sequencing.
442
443 **Anti-serum and antibodies**
444 Mouse anti-Flag (anti-DYKDDDDK tag; Wako 012-22384), rabbit anti-Mei5 serum
445 (Hayase et al., 2004), and anti-tubulin (MCA77G, Bio-Rad/Serotec, Ltd) were
446 used for western blotting. Guinea pig anti-Rad51 (M. Shinohara, Gasior, Bishop,
447 & Shinohara, 2000), rabbit anti-Rfa2 (Hayase et al., 2004), rabbit anti-Dmc1
448 (Sasanuma et al., 2013), and rabbit anti-Mei5 serum (Hayase et al., 2004) were
449 used for staining. With a higher background, IgG was purified using the IgG
450 purification kit (APK-10A, Cosmo Bio co. Ltd). The secondary antibodies for
451 staining were Alexa-488 (Goat) and -594 (Goat) IgG used at a 1/2000 dilution
452 (Themo Fishers).
453
454 **Meiotic Time course**
455 *Saccharomyces cerevisiae* cells were patched onto YPG plates (2%
456 bacteriological peptone, 1% yeast extract, 3% glycerol, 2% agar) and incubated
457 at 30 °C for 12 h. Cells were spread into YPD plates (2% bacteriological peptone,
458 1% yeast extract, 2% glucose, 2% agar) and grown for 48 h to isolate a single
459 colony. The single colony was inoculated into YPD liquid medium and grown to

460 saturation at 30 °C overnight. To synchronize cell cultures, the overnight cultures
461 were transferred to a SPS medium (1% potassium acetate, 1% bacteriological
462 peptone, 0.5% yeast extract, 0.17% yeast nitrogen base with ammonium sulfate
463 and without amino acids, 0.5% ammonium sulfate, 0.05 M potassium biphthalate)
464 and cells were grown for 16–17 h. Meiosis was induced by transferring the SPS-
465 cultured cells to a pre-warmed SPM medium (1% potassium acetate, 0.02%
466 raffinose). The cells were collected at various times after transferring to the SPM
467 medium.
468
469 **Immuno-staining**
470 Immunostaining of chromosome spreads was performed as described previously
471 (M. Shinohara et al., 2000; M. Shinohara, Sakai, Ogawa, & Shinohara, 2003).
472 Briefly, yeast spheroplasts were burst in the presence of 1% paraformaldehyde
473 and 0.1% lipsol. Stained samples were observed using an epi-fluorescent
474 microscope (BX51; Olympus/Evident) with a 100 X objective (NA1.3). Images
475 were captured by CCD camera (Cool Snap; Roper) and, then processed using
476 iVision (Sillicon), and Photoshop (Adobe) software. For focus counting, ~30
477 nuclei were counted at each time point.
478
479 **Western blotting**
480 Western blotting was performed for cell lysates extracted by the TCA method as
481 described (Hayase et al., 2004; M. Shinohara, Oh, Hunter, & Shinohara, 2008).
482 After harvesting and washing twice with 20% TCA, cells were roughly disrupted
483 with zirconia beads (Zircona Y2B05) by the Multi-beads shocker (Yasui Kikai Co
484 Ltd, Japan). Protein precipitates recovered by centrifugation was suspended in
485 SDS-PAGE sample buffer (pH 8.8) and then boiled at 95°C for 10 min. After the
486 electrophoresis, the proteins were transferred onto the Nylon membrane
487 (Immobilon-P, Millipore) and incubated with primary antibodies in a blocking
488 buffer (1X TBS, 0.5% BSA) and then alkaline phosphatase-conjugated secondary
489 antibody (Promega, US). The color reaction was developed with NBT/BCIP
490 solution (Nacalai Tesque, Japan).
491
492 **Pulsed-field gel electrophoresis**
493 For pulsed-field gel electrophoresis (PFGE), chromosomal DNA was prepared in
494 agarose plugs as described in (Bani Ismail, Shinohara, & Shinohara, 2014) and
495 run at 14 °C in a CHEF DR-III apparatus (BioRad) using the field 6V/cm at a

496 120° angle. Switching times followed a ramp from 15.1 to 25.1 seconds. The
497 duration of electrophoresis was 41 h for all chromosomes. For short
498 chromosomes, 5 to 30 seconds and others for 20 to 60 seconds.
499
500 **Immuno-precipitation**
501 Yeast cells were resuspended in the Lysis buffer (50 mM HEPES-NaOH [pH 7.5],
502 140 mM NaCl, 10% Glycerol, 1 mM EDTA, 5% NP-40). An equal amount of
503 zirconia beads (Zircona Y2B05) was added along with the Protease inhibitor
504 cocktail 10X: Roche "Complete™, Mini, EDTA-free Protease Inhibitor Cocktail";
505 4693159001. The cells were disrupted using the Multi-beads shocker (Yasui Kiki;
506 2300 rpm, 60 sec on; 60 sec off cycle, 4 times). The lysates were incubated with
507 magnetic beads (Dynal M260 Protein-A conjugated; GE Healthcare) coated with
508 the anti-Mei5 antibody (6 μl serum in 100 μl beads) at 4 °C for 12 h and washed
509 extensively (Sasanuma et al., 2013). Bound proteins were eluted by adding the
510 SDS sample buffer and were analyzed on an SDS-PAGE gel, transferred to a
511 nylon membrane (Millipore Co. Ltd), and probed with specific antibodies.
512
513 **Protein expression in *E. coli***
514 The expression plasmid for Mei5-R117A-Sae3 was generated from pET21a-
515 Mei5-Sae3 (Hayase et al., 2004) by PCR amplification and Gibson assembly
516 method using primers (5'-
517 CTTTAATCAAAATCAATGCAATGGGCGGCTATAAAGAT-3' and 5'-
518 ATCTTTATAGCCGCCCATTGCATTGATTTTGATTAAAG-3'). Resulting pET21a-
519 Mei5-R117A-Sae3 plasmid was introduced into BL21(DE3) with pLysS and the
520 protein expression was induced at 30°C for 3 h by the addition of IPTG (final 1
521 mM). The protein expression in whole cell lysate was analyzed by SDS-PAGE
522 followed by CBB staining or Western blotting.
523
524 **Software and Statistics**
525 Figures for protein structure analysis were generated by PyMOL. Means ± S.D
526 values are shown. Datasets (focus number) were compared using the Mann-
527 Whitney *U*-test (Prism, GraphPad).
528
529 **Acknowledgments**
530 We are grateful to members of the Shinohara lab. S.M.W., O. P. O., and P.S. was
531 supported by a Japanese government scholarship and by the Institute for Protein

Research. This work was supported by Osaka Fermentation Foundation to A.S.

Competing interest

The authors declare no competing financial interest.

Author contributions

A.S. conceived and designed the experiments. S.M.W. and P.S. carried out strain construction of all yeast experiments. O.P.O. constructed some strains. A.F. expressed proteins. S.M.W., P.S., Y.F., M.I., and A.S. analyzed the data. A.S. wrote the manuscript with inputs from others.

543 **References**

544

545 Akamatsu, Y., Dziadkowiec, D., Ikeguchi, M., Shinagawa, H., & Iwasaki, H. (2003).
546 Two different Swi5-containing protein complexes are involved in mating-
547 type switching and recombination repair in fission yeast. *Proc Natl Acad*
548 *Sci U S A, 100*(26), 15770-15775. doi:10.1073/pnas.2632890100

549 Akamatsu, Y., Tsutsui, Y., Morishita, T., Siddique, M. S., Kurokawa, Y., Ikeguchi,
550 M., . . . Iwasaki, H. (2007). Fission yeast Swi5/Sfr1 and Rhp55/Rhp57
551 differentially regulate Rhp51-dependent recombination outcomes. *EMBO*
552 *J, 26*(5), 1352-1362. doi:10.1038/sj.emboj.7601582

553 Bani Ismail, M., Shinohara, M., & Shinohara, A. (2014). Dot1-dependent histone
554 H3K79 methylation promotes the formation of meiotic double-strand
555 breaks in the absence of histone H3K4 methylation in budding yeast. *PLoS*
556 *One, 9*(5), e96648. doi:10.1371/journal.pone.0096648

557 Bhagwat, N. R., Owens, S. N., Ito, M., Boinapalli, J. V., Poa, P., Ditzel, A., . . .
558 Hunter, N. (2021). SUMO is a pervasive regulator of meiosis. *Elife, 10*.
559 doi:10.7554/eLife.57720

560 Bhattacharya, S., Shcherbik, N., Vasilescu, J., Smith, J. C., Figeys, D., & Haines,
561 D. S. (2009). Identification of lysines within membrane-anchored
562 Mga2p120 that are targets of Rsp5p ubiquitination and mediate
563 mobilization of tethered Mga2p90. *J Mol Biol, 385*(3), 718-725.
564 doi:10.1016/j.jmb.2008.11.018

565 Bishop, D. K., Park, D., Xu, L., & Kleckner, N. (1992). DMC1: a meiosis-specific
566 yeast homolog of E. coli recA required for recombination, synaptonemal
567 complex formation, and cell cycle progression. *Cell, 69*(3), 439-456.
568 Retrieved from
569 http://www.ncbi.nlm.nih.gov/entrez/query.fcgi?cmd=Retrieve&db=PubMe
570 d&dopt=Citation&list_uids=1581960

571 Borner, G. V., Hochwagen, A., & MacQueen, A. J. (2023). Meiosis in budding
572 yeast. *Genetics, 225*(2). doi:10.1093/genetics/iyad125

573 Cejka, P., Mojas, N., Gillet, L., Schar, P., & Jiricny, J. (2005). Homologous
574 recombination rescues mismatch-repair-dependent cytotoxicity of S(N)1-
575 type methylating agents in S. cerevisiae. *Curr Biol, 15*(15), 1395-1400.
576 doi:10.1016/j.cub.2005.07.032

577 Chan, Y. L., Zhang, A., Weissman, B. P., & Bishop, D. K. (2019). RPA resolves
578 conflicting activities of accessory proteins during reconstitution of Dmc1-

mediated meiotic recombination. *Nucleic Acids Res, 47*(2), 747-761. doi:10.1093/nar/gky1160

Chi, P., Kwon, Y., Moses, D. N., Seong, C., Sehorn, M. G., Singh, A. K., . . . Sung, P. (2009). Functional interactions of meiotic recombination factors Rdh54 and Dmc1. *DNA Repair (Amst), 8*(2), 279-284. doi:10.1016/j.dnarep.2008.10.012

Cloud, V., Chan, Y. L., Grubb, J., Budke, B., & Bishop, D. K. (2012). Rad51 is an accessory factor for Dmc1-mediated joint molecule formation during meiosis. *Science, 337*(6099), 1222-1225. doi:10.1126/science.1219379

Ferrari, S. R., Grubb, J., & Bishop, D. K. (2009). The Mei5-Sae3 protein complex mediates Dmc1 activity in Saccharomyces cerevisiae. *J Biol Chem, 284*(18), 11766-11770. doi:10.1074/jbc.C900023200

Haruta, N., Akamatsu, Y., Tsutsui, Y., Kurokawa, Y., Murayama, Y., Arcangioli, B., & Iwasaki, H. (2008). Fission yeast Swi5 protein, a novel DNA recombination mediator. *DNA Repair (Amst), 7*(1), 1-9. doi:10.1016/j.dnarep.2007.07.004

Haruta, N., Kurokawa, Y., Murayama, Y., Akamatsu, Y., Unzai, S., Tsutsui, Y., & Iwasaki, H. (2006). The Swi5-Sfr1 complex stimulates Rhp51/Rad51- and Dmc1-mediated DNA strand exchange in vitro. *Nat Struct Mol Biol, 13*(9), 823-830. doi:10.1038/nsmb1136

Hayase, A., Takagi, M., Miyazaki, T., Oshiumi, H., Shinohara, M., & Shinohara, A. (2004). A protein complex containing Mei5 and Sae3 promotes the assembly of the meiosis-specific RecA homolog Dmc1. *Cell, 119*(7), 927-940. Retrieved from http://www.ncbi.nlm.nih.gov/entrez/query.fcgi?cmd=Retrieve&db=PubMed&dopt=Citation&list_uids=15620352

Hoppe, T., Matuschewski, K., Rape, M., Schlenker, S., Ulrich, H. D., & Jentsch, S. (2000). Activation of a membrane-bound transcription factor by regulated ubiquitin/proteasome-dependent processing. *Cell, 102*(5), 577-586. doi:10.1016/s0092-8674(00)00080-5

Hunter, N. (2015). Meiotic Recombination: The Essence of Heredity. *Cold Spring Harb Perspect Biol, 7*(12). doi:10.1101/cshperspect.a016618

Jumper, J., Evans, R., Pritzel, A., Green, T., Figurnov, M., Ronneberger, O., . . . Hassabis, D. (2021). Highly accurate protein structure prediction with AlphaFold. *Nature, 596*(7873), 583-589. doi:10.1038/s41586-021-03819-2

Kokabu, Y., Murayama, Y., Kuwabara, N., Oroguchi, T., Hashimoto, H., Tsutsui, Y., . . . Ikeguchi, M. (2011). Fission yeast Swi5-Sfr1 protein complex, an activator of Rad51 recombinase, forms an extremely elongated dogleg-shaped structure. *J Biol Chem, 286*(50), 43569-43576. doi:10.1074/jbc.M111.303339

Kuwabara, N., Murayama, Y., Hashimoto, H., Kokabu, Y., Ikeguchi, M., Sato, M., . . . Shimizu, T. (2012). Mechanistic insights into the activation of Rad51-mediated strand exchange from the structure of a recombination activator, the Swi5-Sfr1 complex. *Structure, 20*(3), 440-449. doi:10.1016/j.str.2012.01.005

Lan, W. H., Lin, S. Y., Kao, C. Y., Chang, W. H., Yeh, H. Y., Chang, H. Y., . . . Li, H. W. (2020). Rad51 facilitates filament assembly of meiosis-specific Dmc1 recombinase. *Proc Natl Acad Sci U S A, 117*(21), 11257-11264. doi:10.1073/pnas.1920368117

Li, P., Jin, H., Koch, B. A., Abblett, R. L., Han, X., Yates, J. R., 3rd, & Yu, H. G. (2017). Cleavage of the SUN-domain protein Mps3 at its N-terminus regulates centrosome disjunction in budding yeast meiosis. *PLoS Genet, 13*(6), e1006830. doi:10.1371/journal.pgen.1006830

Lu, C. H., Yeh, H. Y., Su, G. C., Ito, K., Kurokawa, Y., Iwasaki, H., . . . Li, H. W. (2018). Swi5-Sfr1 stimulates Rad51 recombinase filament assembly by modulating Rad51 dissociation. *Proc Natl Acad Sci U S A, 115*(43), E10059-E10068. doi:10.1073/pnas.1812753115

Luo, S. C., Yeh, H. Y., Lan, W. H., Wu, Y. M., Yang, C. H., Chang, H. Y., . . . Tsai, M. D. (2021). Identification of fidelity-governing factors in human recombinases DMC1 and RAD51 from cryo-EM structures. *Nat Commun, 12*(1), 115. doi:10.1038/s41467-020-20258-1

Marston, A. L. (2014). Chromosome segregation in budding yeast: sister chromatid cohesion and related mechanisms. *Genetics, 196*(1), 31-63. doi:10.1534/genetics.112.145144

Ogawa, T., Yu, X., Shinohara, A., & Egelman, E. H. (1993). Similarity of the yeast RAD51 filament to the bacterial RecA filament. *Science, 259*(5103), 1896-1899. doi:10.1126/science.8456314

Sasanuma, H., Tawaramoto, M. S., Lao, J. P., Hosaka, H., Sanda, E., Suzuki, M., . . . Shinohara, A. (2013). A new protein complex promoting the assembly of Rad51 filaments. *Nat Commun, 4*, 1676. doi:10.1038/ncomms2678

Sawant, P., Mwaniki, S., Fujita, Y., Ito, M., Furukohri, A., & Shinohara, A. (2023). The role of conserved amino acid residues of Sae3 in Mei5-Sae3 complex for Dmc1 assembly in meiotic recombination. *Genes Genet Syst, 98*(1), 45-52. doi:10.1266/ggs.23-00015

Say, A. F., Ledford, L. L., Sharma, D., Singh, A. K., Leung, W. K., Sehorn, H. A., . . . Sehorn, M. G. (2011). The budding yeast Mei5-Sae3 complex interacts with Rad51 and preferentially binds a DNA fork structure. *DNA Repair (Amst), 10*(6), 586-594. doi:10.1016/j.dnarep.2011.03.006

Shinohara, A., Ogawa, H., & Ogawa, T. (1992). Rad51 protein involved in repair and recombination in S. cerevisiae is a RecA-like protein. *Cell, 69*(3), 457-470. Retrieved from http://www.ncbi.nlm.nih.gov/entrez/query.fcgi?cmd=Retrieve&db=PubMed&dopt=Citation&list_uids=1581961

Shinohara, A., & Ogawa, T. (1998). Stimulation by Rad52 of yeast Rad51-mediated recombination. *Nature, 391*(6665), 404-407. doi:10.1038/34943

Shinohara, M., Gasior, S. L., Bishop, D. K., & Shinohara, A. (2000). Tid1/Rdh54 promotes colocalization of rad51 and dmc1 during meiotic recombination. *Proc Natl Acad Sci U S A, 97*(20), 10814-10819. Retrieved from http://www.ncbi.nlm.nih.gov/entrez/query.fcgi?cmd=Retrieve&db=PubMed&dopt=Citation&list_uids=11005857

Shinohara, M., Oh, S. D., Hunter, N., & Shinohara, A. (2008). Crossover assurance and crossover interference are distinctly regulated by the ZMM proteins during yeast meiosis. *Nat Genet, 40*(3), 299-309. Retrieved from http://www.ncbi.nlm.nih.gov/entrez/query.fcgi?cmd=Retrieve&db=PubMed&dopt=Citation&list_uids=18297071

Shinohara, M., Sakai, K., Ogawa, T., & Shinohara, A. (2003). The mitotic DNA damage checkpoint proteins Rad17 and Rad24 are required for repair of double-strand breaks during meiosis in yeast. *Genetics, 164*(3), 855-865. doi:10.1093/genetics/164.3.855

Su, G. C., Chung, C. I., Liao, C. Y., Lin, S. W., Tsai, C. T., Huang, T., . . . Chi, P. (2014). Enhancement of ADP release from the RAD51 presynaptic filament by the SWI5-SFR1 complex. *Nucleic Acids Res, 42*(1), 349-358. doi:10.1093/nar/gkt879

Sung, P. (1997). Yeast Rad55 and Rad57 proteins form a heterodimer that functions with replication protein A to promote DNA strand exchange by Rad51 recombinase. *Genes Dev, 11*(9), 1111-1121.

doi:10.1101/gad.11.9.1111

Tsai, S. P., Su, G. C., Lin, S. W., Chung, C. I., Xue, X., Dunlop, M. H., . . . Chi, P. (2012). Rad51 presynaptic filament stabilization function of the mouse Swi5-Sfr1 heterodimeric complex. *Nucleic Acids Res, 40*(14), 6558-6569. doi:10.1093/nar/gks305

Tsubouchi, H., & Roeder, G. S. (2004). The budding yeast mei5 and sae3 proteins act together with dmc1 during meiotic recombination. *Genetics, 168*(3), 1219-1230. doi:10.1534/genetics.103.025700

Xu, J., Zhao, L., Peng, S., Chu, H., Liang, R., Tian, M., . . . Wang, H. W. (2021). Mechanisms of distinctive mismatch tolerance between Rad51 and Dmc1 in homologous recombination. *Nucleic Acids Res, 49*(22), 13135-13149. doi:10.1093/nar/gkab1141

701 **Figure legends:**

702

703 **Figure 1. Predicted Mei5 structure and the relationship with Swi5-Sfr1.**

704 A. Predicted structure of the budding yeast Mei5 (gray) by the AlphaFold2
705 (https://alphafold.ebi.ac.uk); AF-P32489. The amino acid residues studied in
706 this study are shown as a stick with a color. The disordered N-terminal region
707 (1-45) of Mei5 is deleted in the schematic model.

708 B. Structural comparison of a predicted Mei5 (gray; 46-221) with a C-terminal
709 region of fission yeast Sfr1(green; 178-299; PDB, 3viq) complex. The
710 structure alignment was performed by PyMOL.

711 C. The entry into meiosis I in various strains was analyzed by DAPI staining. The
712 number of DAPI bodies in a cell was counted. A cell with 2, 3, and 4 DAPI
713 bodies was defined as a cell that passed through meiosis I. The graph shows
714 the percentages of cells that completed MI or MII at the indicated time points.
715 Strains used are as follows: Wild-type, MSY832/833; *mei5*::*URA3*, PSY64/65;
716 *mei5-K51A R58A*, PSY33/34; *mei5-R68A K79A*, PSY23/24; *mei5-K95A*,
717 PSY11/12; *mei5-K95L*, PSY123/124; *mei5-R97A*, PSY15/16; *mei5-R97L*,
718 PSY13/14; *mei5-K114A*, PSY33/34; *mei5-R117A*, PSY78/79. More than 100
719 cells were counted at each time point.

720 D. Expression of various mutant Mei5 proteins during meiosis. Lysates obtained
721 from the cells at various time points during meiosis were analyzed by western
722 blotting using anti-Mei5 (upper) or anti-tubulin (lower) antibodies.

723

724 **Figure 2. *mei5* mutations cause defective in Dmc1 assembly**

725 A. Rad51 and Dmc1 staining. Nuclear spreads were stained with anti-Rad51
726 (green) and anti-Dmc1 (red). Representative images at each time point under
727 the two conditions are shown. Strains used are as follows: Wild-type,
728 NKY1551; *mei5::URA3* deletion, PSY5/6; *mei5-K95L*, PSY133/137; *mei5-*
729 *R97A*, PSY86/90; *mei5-R97L*, PSY131/141. Bar = 2 μm.

730 B. Rad51 and Mei5 staining. Nuclear spreads were stained with anti-Rad51 (red)
731 and anti-Mei5 (green). Representative images at each time point under the
732 two conditions are shown. Bar = 2 μm.

733 C. Kinetics of assembly/disassembly of Rad51, Dmc1, Rfa2 and Mei5. The
734 number of cells positive for foci (with more than 5 foci) was counted at each
735 time point. At each time point, more than 100 cells were counted. The average
736 values and SDs of triplicates are shown.

737 D. The number of foci of Rad51, Dmc1, Rfa2, and Mei5 at 4 h was manually
738 counted. The graphs show the focus number combined from three
739 independent time courses. On the top, an average focus number in positive
740 nucleus is shown. Error bars (green) is a mean with standard deviation.
741
742 **Figure 3. The *mei5-R97A* and *-R97L* are defective in Dmc1-assembly**
743 A. Rad51 and Dmc1 staining. Nuclear spreads of *SAE3-Flag* cells with various
744 *mei5* mutations were stained with anti-Rad51 (green) and anti-Dmc1 (red).
745 Representative images at each time point under the two conditions are
746 shown. Strains with *SAE3-FLAG* used are as follows: Wild-type, PSY31/32;
747 *mei5::URA3* deletion, PSY166/167; *mei5-K95L*, PSY144/148; *mei5-R97L*,
748 PSY157/158. Bar = 2 μm.
749 B. Mei5 and Sae3 staining. Nuclear spreads were stained with anti-Rad51
750 (green), anti-Flag (Sae3, red), and, in some cases, DAPI (blue).
751 Representative images at each time point under the two conditions are shown.
752 Bar = 2 μm.
753 C. Kinetics of assembly/disassembly of Rad51, Dmc1, Mei5 and Sae3. The
754 number of cells positive for foci (with more than 5 foci) was counted at each
755 time point. At each time point, more than 100 cells were counted. The average
756 values and SDs of triplicates are shown.
757 D. The number of foci of Rad51 and Dmc1 at 4 h was manually counted. The
758 graphs show the focus number combined from three independent time
759 courses. On the top, an average focus number in positive nucleus is shown.
760 Error bars (green) is a mean with standard deviation.
761 E. IP of Sae3-Flag by anti-Mei5 serum. IP fractions of meiotic lysates at 4 h from
762 various strains were probed with anti-Mei5 (top) or anti-Flag (bottom). Strains
763 used are as follows: *SAE3-Flag*, PSY31/32; *mei5-K95L SAE3-Flag*,
764 PSY144/148; *mei5-R97L SAE3-Flag*, PSY157/158.
765
766 **Figure 4. The *mei5-R117A* is defective in Dmc1 assembly**
767 A. Rad51/Dmc1 staining in WT and *mei5-R117A* mutant cells. Nuclear spreads
768 were stained with anti-Rad51 (green), and anti-Dmc1 (red). Representative
769 images at each time point under the two conditions are shown. Strains used
770 are as follows: Wild-type, NKY1551; *mei5-R117A*, SMY192/195. Bar = 2 μm.
771 B. Mei5 staining. Nuclear spreads were stained with anti-Mei5 (green) and DAPI
772 (blue). Representative images at each time point under the two conditions are

773 shown. Bar = 2 μm.
774 C. Kinetics of Rad51/Dmc1/Mei5 foci in WT and *mei5-R117A* mutant cells. The
775 number of cells positive for foci (with more than 5 foci) was counted at each
776 time point. At each time point, more than 100 cells were counted. The average
777 values and SDs of triplicates are shown.
778
779 **Figure 5. Mei5-R117A produces a truncated protein**
780 A. Expression of Mei5-R117A. Cell lysates at each time were verified by western
781 blotting with anti-Mei5 and anti-tubulin (control). Representative blots in
782 duplicate are shown. Strains used are as follows: Wild-type, NKY1551; *mei5-*
783 *R117A*, SMY192/195. A red arrowhead indicates a possible processed form
784 of wild-type Mei5 protein.
785 B. Expression of Mei5-R117A-3xFlag protein. Lysates of cell with Mei5-Flag or
786 Mei5-R117A-Flag at each time were verified by western blotting with anti-Flag
787 (left panel) anti-Mei5 (right panel), and anti-tubulin (bottom right). As a control,
788 cells without the Flag tag on Mei5 were analyzed (right three lanes).
789 Representative blots in duplicate are shown. Strains used are as follows: Wild-
790 type with Mei5-Flag, SMY209/212; *mei5-R117A-Flag*, SMY210/222; Wild-
791 type, NKY1551; *mei5-R117A*, SMY192/195. An asterisk means non-specific
792 band cross-reacted with anti-Flag, which appear in late prophase I. Red
793 arrowheads indicate a possible processed form of wild-type Mei5 protein.
794 C. Expression of Mei5-R117A *in E. coli* cells. Cell lysates with or without the
795 protein induction (with IPTG) were verified by western blotting with anti-Mei5.
796 A representative blot in duplicate is shown. Vector, pET21a; wild-type,
797 pET21a-Mei5-Sae3; pET21a-Mei5(R117A)-Sae3. Yeast lysates from wild-
798 type and *mei5-R117A* were analyzed as a control (two right lanes).
799
800 **Figure 6. Mei5-R117A is processed post-translationally**
801 A. Schematic drawing of Mei5 C-terminal deletion mutants; *mei5-d(190-221)* and
802 *mei5-d(197-221)*. Gray rectangles present putative α-helixes (see Figure 1A).
803 B. Expression of *mei5* C-terminal deletion mutants. Yeast cell lysates at each
804 time were verified by western blotting (bottom) with anti-Mei5, and anti-tubulin
805 (control). Representative blots in duplicate are shown. Strains used are as
806 follows: Wild-type, NKY1551; *mei5-R117A*, SMY192/195; *mei5-d(190-221)*,
807 SMY343/345; *mei5-d(197-221)*, SMY270/272.
808 C. The entry into meiosis I in *mei5* C-terminal deletion mutant cells was analyzed

809 by DAPI staining. The number of DAPI bodies in a cell was counted. A cell
810 with 2, 3, and 4 DAPI bodies was defined as a cell that passed through meiosis
811 I. The graph shows the percentages of cells that completed MI or MII at the
812 indicated time points. Wild-type, NKY1551; *mei5-R117A*, SMY192/195; *mei5-*
813 *R117K*, SMY249/251; *mei5-R117E*, SMY253/255.
814 D. Expression of the various Mei5-R117 mutant proteins. Representative blots in
815 duplicate are shown. Strains used are as follows: Wild-type, NKY1551; *mei5-*
816 *R117A*, SMY192/195; *mei5-R117K*, SMY249/251; *mei5-R117E*, SMY253/255.
817 E. The entry into meiosis I in various strains was analyzed by DAPI staining. The
818 average values and SDs of triplicates are shown. Wild-type, NKY1551; *mei5-*
819 *R117A*, SMY192/195; *mei5-d(190-221)*, SMY343/345; *mei5-d(197-221)*,
820 SMY270/272.
821 F. Expression of Mei5-R117A in the *sae3* deletion. Lysates of cells with or
822 without the *SAE3* were verified at each time by western blotting with anti-Mei5
823 and anti-tubulin (control). Representative blots in duplicate are shown. Strains
824 used are as follows: Wild-type, NKY1551; *mei5-R117A*, SMY192/195; *sae3*,
825 SMY261/263; *sae3 mei5-R117A*, SMY265/267.
826 G. Expression of Mei5-R117A in mitotic yeast cells. The expression of Mei5 or
827 Mei5-R117A protein from *GAL1/10* promoter was verified by western blotting.
828 At 0 h, 2% Galactose was added. Note-Gal1/10 did not work efficiently in SK1
829 background. Diploid cells with the expression vector of wild-type Mei5
830 (SMY291/292) and Mei5-R117A (SMY296/297) proteins were used. As a
831 control, meiotic cell lysates of wild-type and *mei5-R117A* mutant cells at 4 h
832 after meiosis induction were analyzed. Representative blots in duplicate are
833 shown.
834
835 **Figure 7. Mei5-K133A shows post-translational processing**
836 A. Predicted structure of the budding yeast Mei5 (gray; 46-221) by the
837 AlphaFold2 (https://alphafold.ebi.ac.uk); AF-P32489. The amino acid
838 residues studied in this study are shown as a stick with a color.
839 B. Expression of Mei5-K133A and -R134A. Cell lysates at each time were
840 verified by western blotting with anti-Mei5 and anti-tubulin (control).
841 Representative blots in duplicate are shown. Strains used are as follows: Wild-
842 type, NKY1551; *mei5-K133A*, SM258/259; *mei5-R134A*, SM280/281.
843
844

Figure 1. Mwaniki et al.

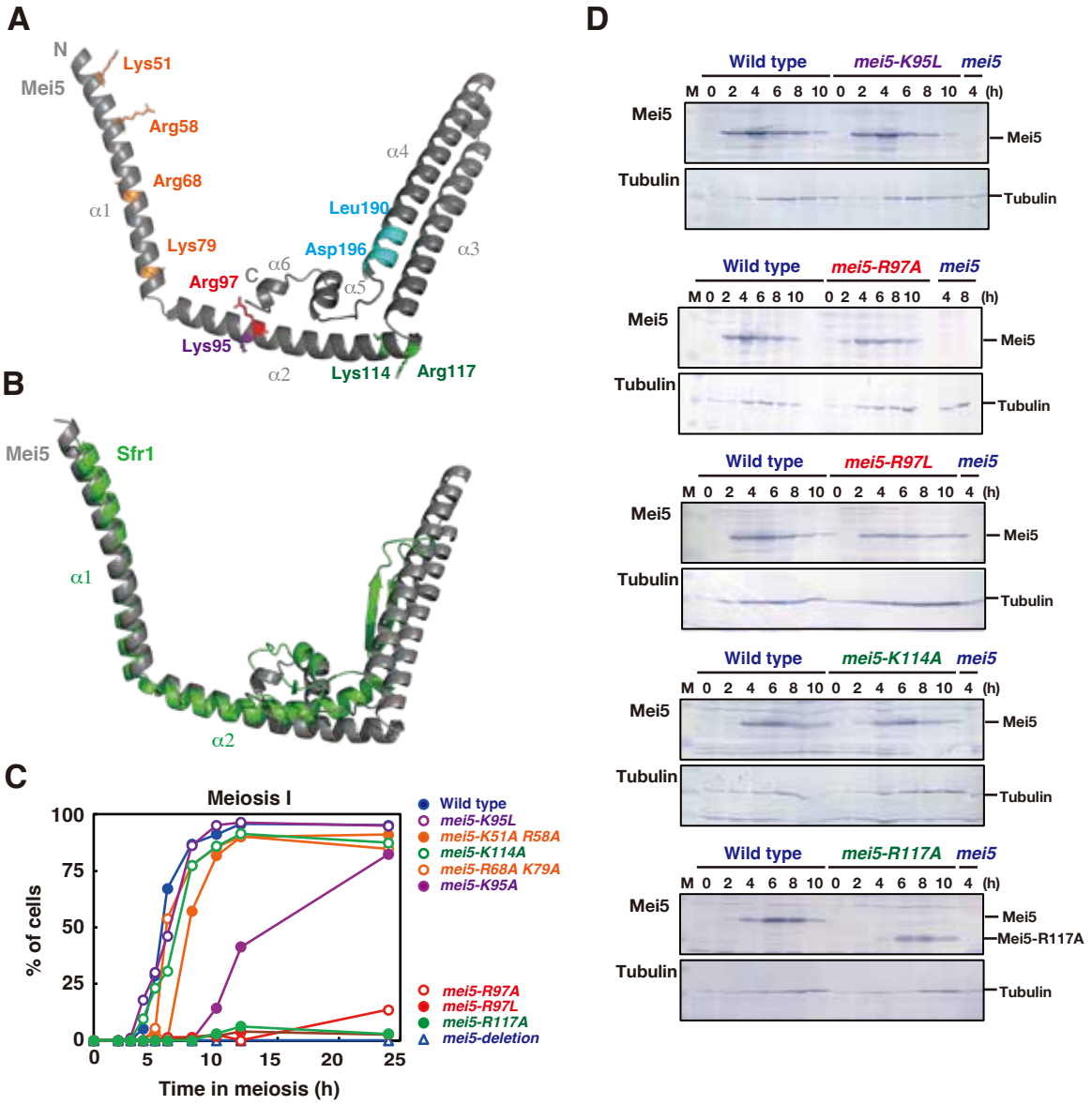

Figure 2. Mwaniki et al.

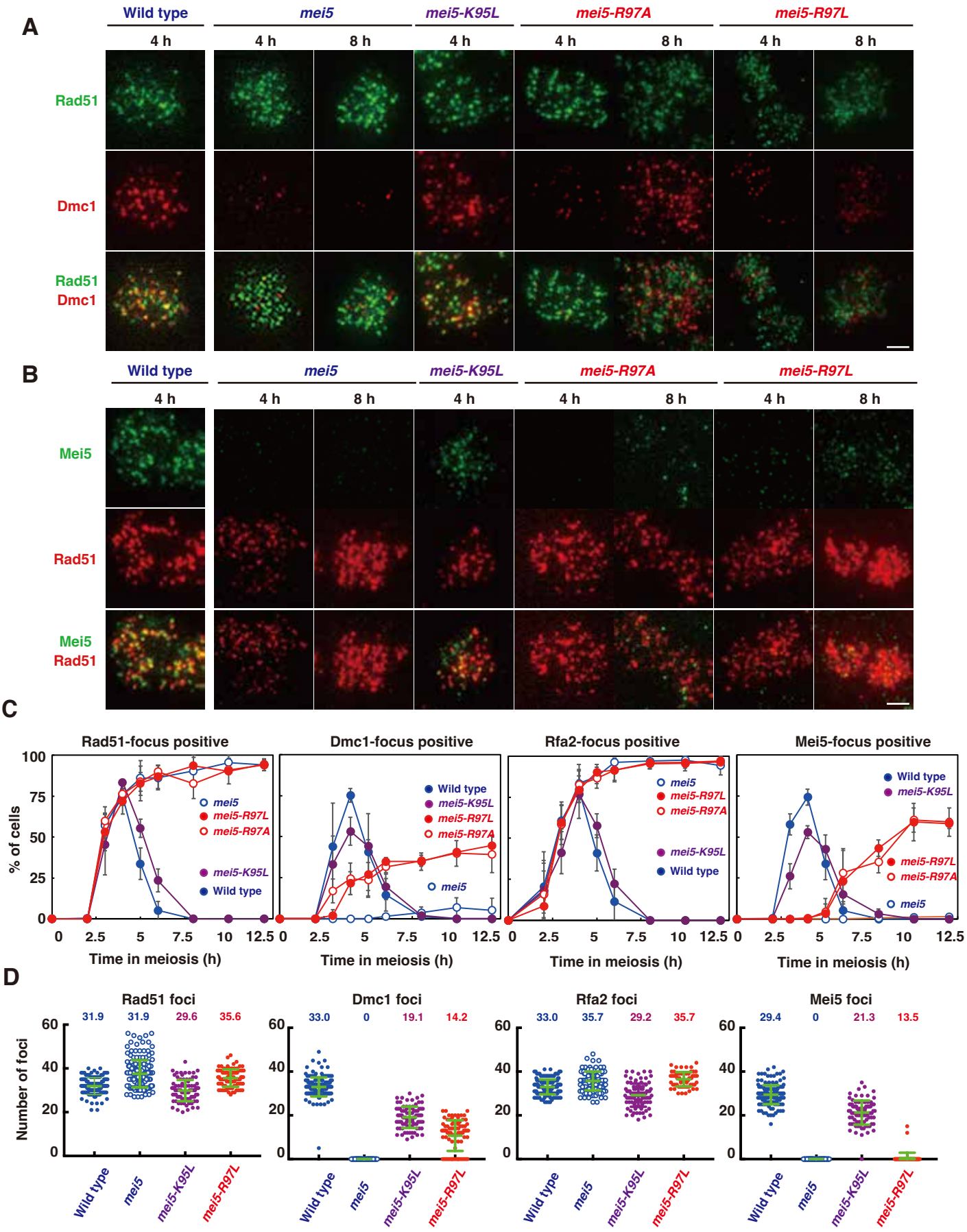

Figure 3. Mwaniki et al.

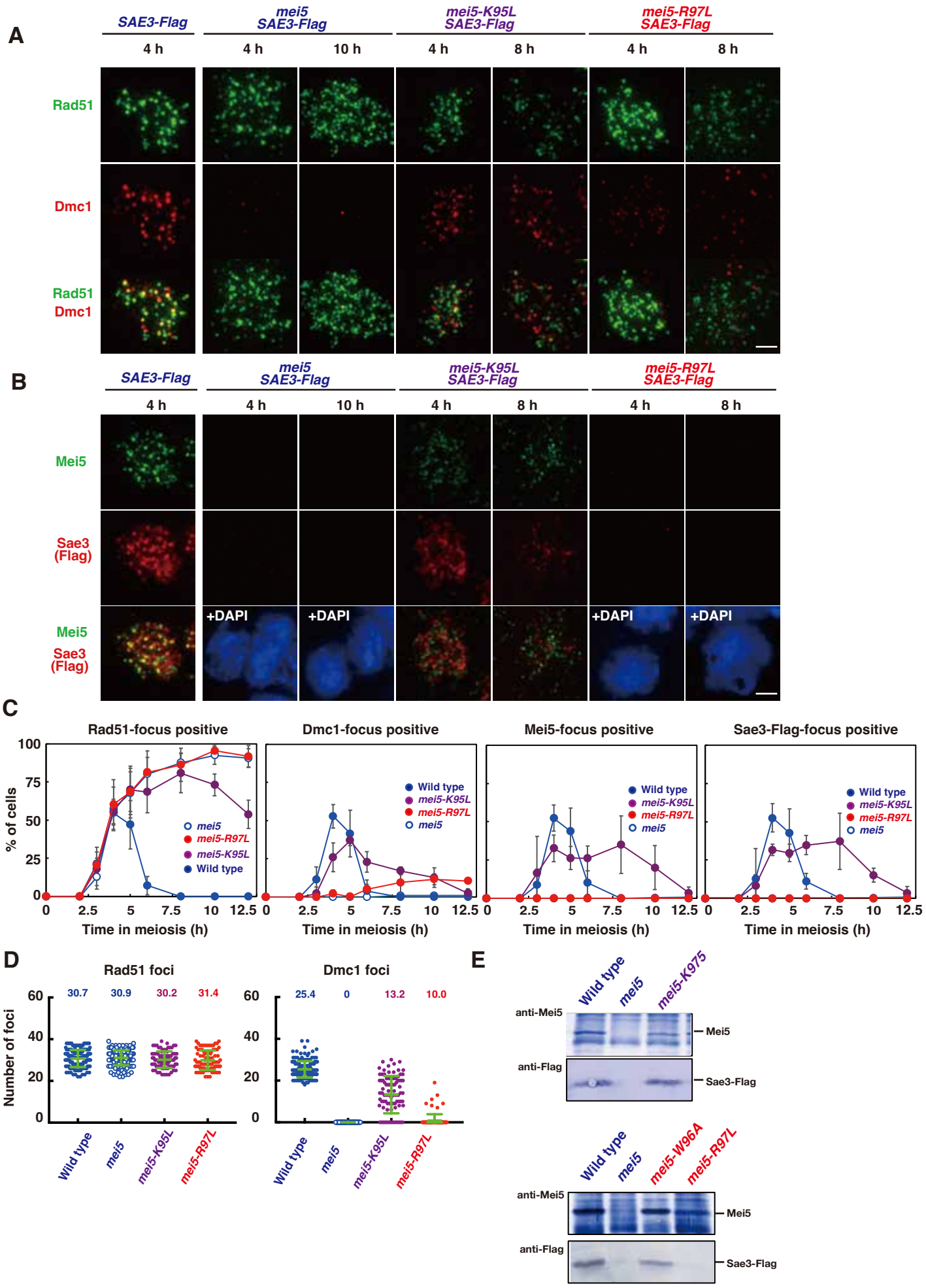

Figure 4. Mwaniki et al.

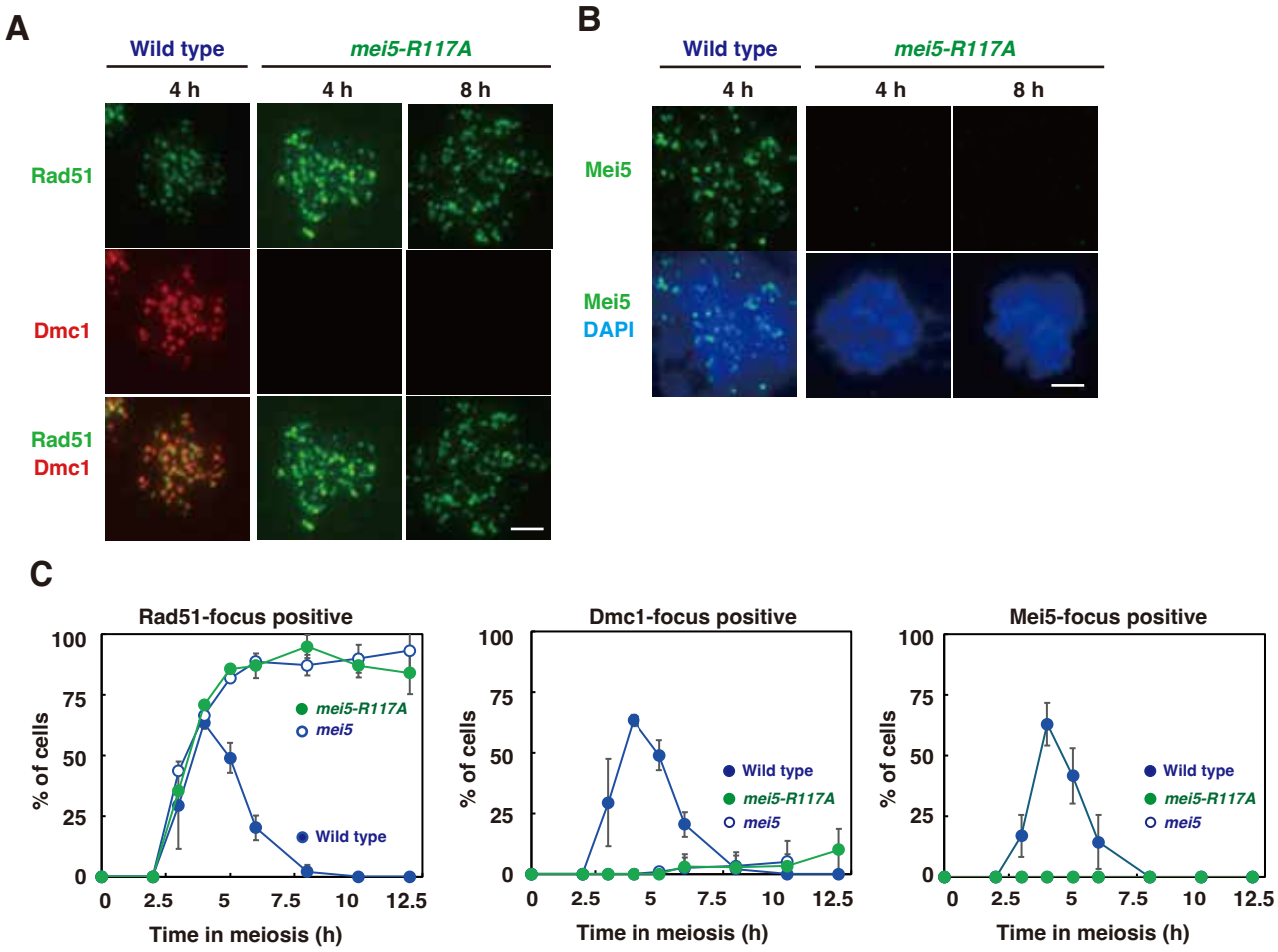

Figure 5. Mwaniki et al.

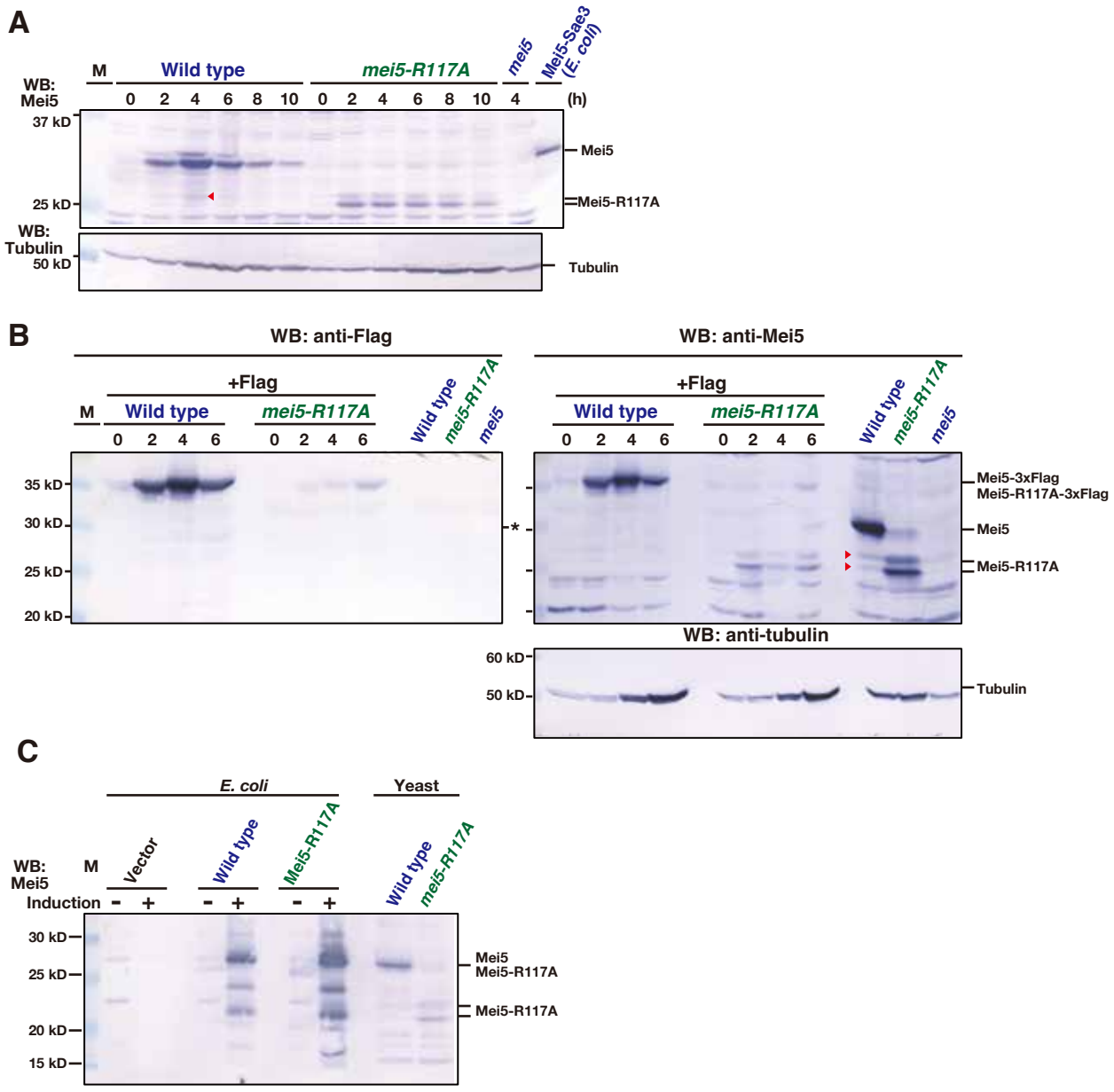

Figure 6. Mwaniki et al.

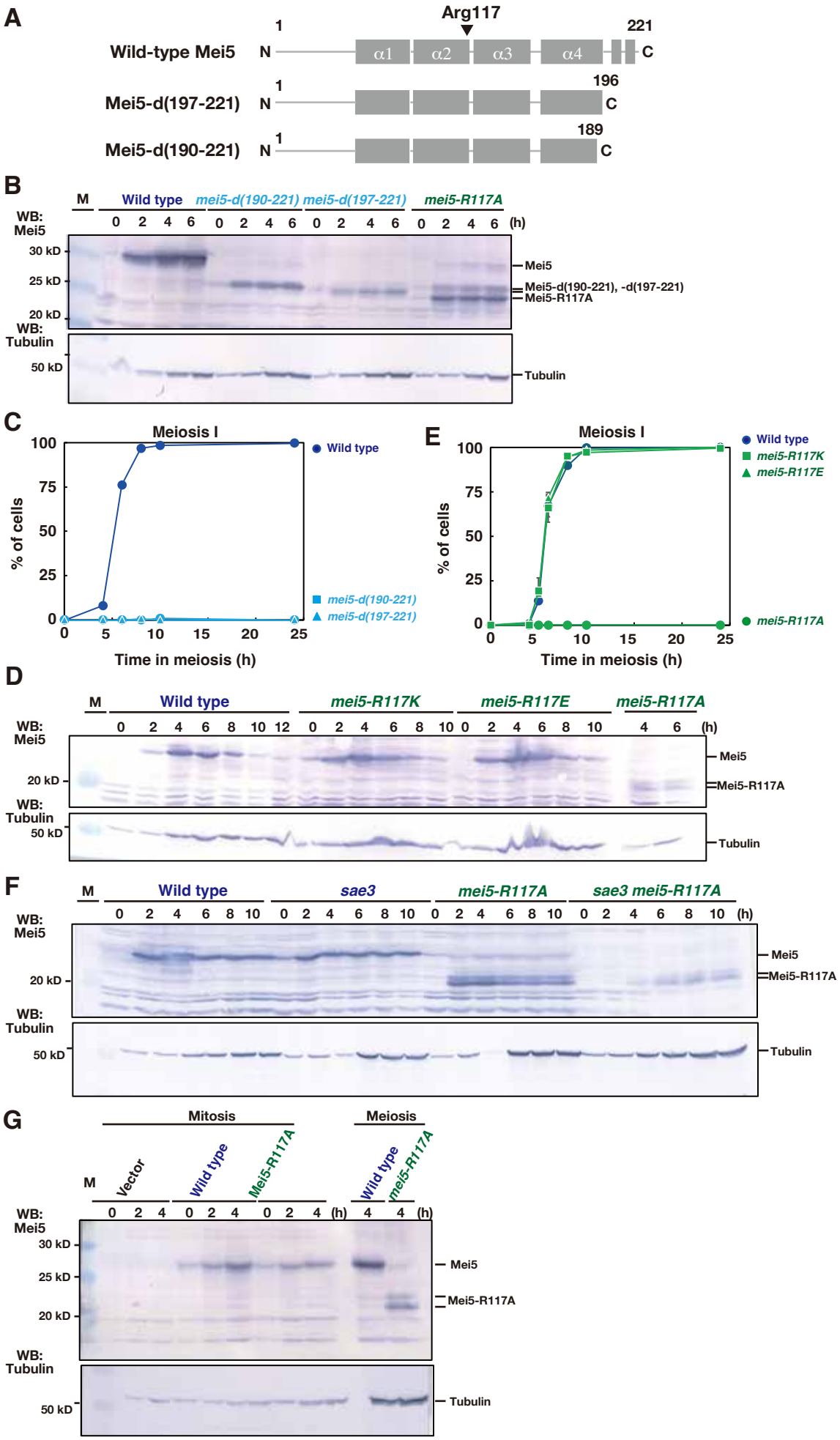

Figure 7. Mwaniki et al.